Residual Amplitude Modulation Reduction in Integrated Indium Phosphide Phase Modulators

Victoria Rosborough[1*], Joseph Fridlander[1], Fengqiao Sang[1], Fabrizio Gambini[1], Simone Tommaso Šuran Brunelli[1], Jeffrey R. Chen[2], Stephan Kawa[2], Kenji Numata[2], Mark Stephen[2], Larry Coldren[1], Jonathan Klamkin[1]

[1]*Electrical and Computer Engineering Department, University of California Santa Barbara, Santa Barbara, CA 93106 USA*
[2]*NASA Goddard Space Flight Center, Greenbelt, MD 20771 USA*
**rosborough@ucsb.edu*

Abstract: A novel indium phosphide Mach-Zehnder interferometer with directional couplers was realized to compensate residual amplitude modulation in integrated phase modulators. The change in transmission for π phase shift was reduced from 3.85 dB to 1.98 dB.
OCIS codes: (130.3120) Integrated optics devices; (130.4110) Modulators

1. Introduction

Low residual amplitude modulation (RAM) phase modulators (PMs) are important for a host of applications, including precision spectroscopy, LIDAR, and quantum communications [1,2]. These applications would also benefit from reduced instrument size, weight, power consumption, and cost. Indium phosphide (InP)-based photonic integrated circuits (PICs) combine lasers, modulators, photodetectors, and passive components such as directional couplers on a single chip, greatly reducing footprint and improving reliability [3,4]. Typical InP PMs, however, suffer from bias-dependent high RAM, thereby motivating novel phase modulator implementations and/or RAM reduction for InP PICs [5].

In this work, we present an adaptation of the shift-and-dump phase shifter (SDPS) that was first demonstrated in silicon [6,7] to InP phase modulators for RAM reduction. The SDPS is a Mach-Zehnder interferometer-based device with directional couplers at the input and output (see top of Fig. 2(a)). By choosing the correct PM length and directional coupler splitting ratios, the device yields an almost constant total loss despite varying loss in the modulated arm as the phase changes. The ideal condition for the SDPS, as given in [6] is:

$$E_{out}\left(\varphi_1 + {}^{j\alpha_1}/_{2}\right) = E_{out}(0)e^{j\varphi_1} \quad (1)$$

With the device configuration shown at the top of Fig. 2(a), eqn. 1 becomes:

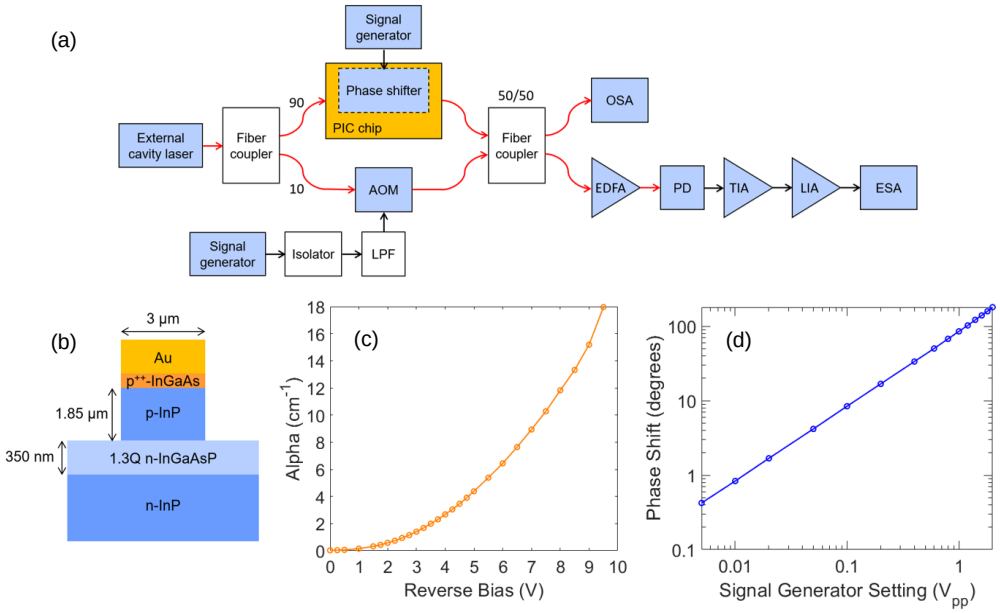

Figure 1. (a) Test setup used to measure straight PM efficiency. LPF = low pass filter, AOM = acousto-optic modulator, OSA = optical spectrum analyzer, EDFA = erbium-doped fiber amplifier, PD = photodiode, TIA = transimpedance amplifier, LIA = lock-in amplifier, ESA = electrical spectrum analyzer. (b) Cross-section of PM. (c) Waveguide loss as a function of reverse bias. (d) Straight PM efficiency.

$$e^{j\varphi_1}\sqrt{(1-\kappa_1)(1-\kappa_2)}\left(1-e^{-\alpha_1 L/2}\right)+e^{\left(j\varphi_2-\alpha_2 L/2\right)}\sqrt{\kappa_1\kappa_2}\left(1-e^{j\varphi_1}\right)=0 \quad (2)$$

where φ_1 and α_1 are the maximum phase shift and corresponding loss on the modulated arm and φ_2 is a constant bias applied to the top arm with accompanying loss α_2.

2. Straight Phase Modulator Characterization

To determine optimal values for the directional coupler splitting ratios, κ_1 and κ_2, and the SDPS arm length, L, the waveguide PM loss as a function of reverse bias and modulation efficiency must be determined. A cross-section of the PM waveguide is shown in Fig. 1(b). Phase change is accomplished by the Franz-Keldysh effect in the bulk indium gallium arsenide phosphide (InGaAsP) waveguide layer. To measure the loss as a function of reverse bias, a test structure with an integrated laser followed by a 2.5-mm long PM was used. With the laser on, the photocurrent at the PM was recorded for increasing reverse bias and converted to the loss values shown in Fig. 1(c). The method described in [8] was used to measure the modulation efficiency and the test setup is shown in Fig. 1(a). Figure 1(d) plots the linear component of the Fourier spectrum of the phase modulation and yields a modulation efficiency of approximately 30°/(V·mm). The PM was modulated at 500 kHz around a bias point of -1.5 V.

3. SDPS Design, Fabrication, and Characterization

An optical micrograph of the fabricated SDPS is shown at the bottom of Fig. 2(a). Based on the results from characterizing the straight PM it was determined that $\kappa_1 = \kappa_2 = 0.15$ for an arm length of 816 µm. The splitting ratio of the fabricated directional couplers was measured to be $\kappa = 0.12$. The black line in Fig. 2(b) shows the measured change in transmission through the SDPS as a function of reverse bias up to V_π. The total change in transmission level over π phase shift is 1.98 dB, whereas the expected change in transmission for the equivalent length straight PM, shown in blue, is 3.85 dB, representing almost a 50% decrease. The orange line is the calculated transmission for an SDPS with $\kappa_1 = \kappa_2 = 0.12$ and shows a transmission change of 1.41 dB, demonstrating that our device came close to the achievable transmission flattening.

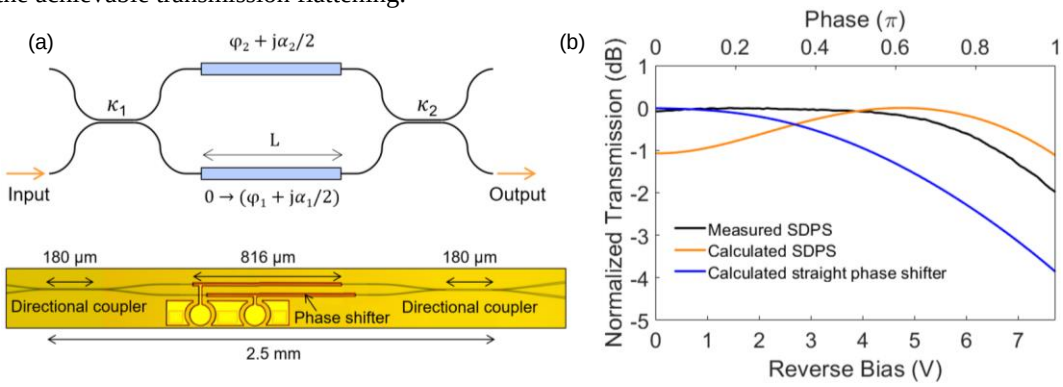

Figure 2. (a) Top: SDPS structure adapted from [6] Bottom: fabricated SDPS. (b) Measured change in transmission with reverse bias for SDPS (black) and expected change in transmission for the SDPS (orange) and straight PM of equivalent length (blue).

4. Conclusion

The device presented in this work reduces RAM in InP PMs by compensating for loss due to electro-absorption. The change in transmission for π phase shift was reduced from 3.85 dB to 1.98 dB for an 816-µm long PM. This implementation represents progress towards integrated laser stabilization for compact remote LIDAR sensors for small form factor satellites.

5. Acknowledgements

The authors acknowledge NASA for support through the ROSES Advanced Component Technology program. A portion of this work was performed in the UCSB Nanofabrication Facility.

6. References

[1] K. Numata, et al., "Frequency stabilization of distributed-feedback laser diodes at 1572 nm for lidar measurements of atmospheric carbon dioxide," *Applied Optics*, **50** (7) 1047—1056 (2011).
[2] P. Sibson, et al., "Integrated silicon photonics for high speed quantum key distribution," *Optica*, **4** (2) 172—177 (2017).
[3] J. Fridlander, et al., "Photonic integrated circuits for precision spectroscopy," presented at CLEO conf., SF30.3, (2020).
[4] V. Rosborough, et al., "Monolithic integration of widely-tunable DBR and DFB lasers with one-step grating formation," presented at OSA Advanced Photonics Congress IPR, IM2A.5, (2019).
[5] S. Andreou, et al., "Steady state analysis of the effects of residual amplitude modulation of InP-based integrated phase modulators in Pound-Drever-Hall frequency stabilization," *IEEE Photonics Journal*, **11** (3) (2019).
[6] N. Dupuis, et al., "Nanosecond-scale shift-and-dump Mach-Zehnder switch," *Optics Letters*, **44** (18) 4614—4616 (2019).
[7] Dupuis et al., "Electro-optic phase modulator with no residual amplitude modulation," US Patent 9912413B1 (2018).
[8] B. Arar, et al., "Method for in-depth characterization of electro-optic phase modulators," *Applied Optics*, **56** (4) 1246—1252 (2017).